switching losses, while the HBa bridge operates at a higher switching frequency, typically in the kHz range.

In general, the switching losses for a single switch can be calculated using the following expression:

$$P_{sw} = \frac{1}{2} V_c I_l f_{sw} \left(t_{on} + t_{off} \right), \quad (8)$$

these losses depend on several factors: V_c which represents the voltage of the compensator feeding the H-bridge of the generic component; I_l the load current; t_{on} and t_{off} the turn-on and turn-off times of the switch; and f_{sw} the switching frequency. This applies to the losses of a single switch; however, to adapt it to the system under consideration, which consists of two cascaded H-bridges, one operating at twice the voltage of the other, the Equation (8) becomes:

$$\begin{aligned} P_{sw\_TOT} = P_{HBa} + P_{HBb} &= \tfrac{1}{2}\, n_c\, V_c I_l f_{sw} \left(t_{on} + t_{off} \right) + \tfrac{1}{2} n_c\, 2\, V_c I_l f_{sw} \left(t_{on} + t_{off} \right) \\ &= \tfrac{1}{2}\, n_c I_l \left(t_{on} + t_{off} \right) V_c (f_{sw} + 2 f_{sw}), \end{aligned} \quad (9)$$

where n_c denotes the number of switches in each H-bridge, which in this case is always equal to 4. The same equation adapted to PD-PWM is:

$$P_{sw\_PWM} = P_{HBa} + P_{HBb} = \frac{3}{2}\, n_c I_l \left(t_{on} + t_{off} \right) V_c f_{PWM}, \quad (10)$$

where f_{PWM} is the switching frequency associated with the PWM technique, which is typically in the order of kHz.

For the SMS technique the (9) became:

$$P_{sw\_SMS} = P_{HBa} + P_{HBb} = 2\, n_c I_l \left(t_{on} + t_{off} \right) V_c f_1, \quad (11)$$

where f_1 is the fundamental frequency, typically a few Hz. The same Equation (9), adapted to proposed hybrid modulation, becomes:

$$P_{sw\_HBR} = P_{HBa} + P_{HBb} = \frac{1}{2}\, n_c I_l \left(t_{on} + t_{off} \right) V_c (f_{PWM} + 2 f_1) \quad (12)$$

In conclusion, it has been demonstrated that the proposed hybrid modulation allows to reduce the switching losses respect to the MC PWM scheme. Therefore:

$$P_{sw\_PWM} > P_{sw\_HBR} > P_{sw\_SMS}, \quad (13)$$

Considering (14), it can be stated that the switching losses of the hybrid technique are higher than those of the SMS technique. Consequently, a converter employing the hybrid technique will inevitably exhibit lower efficiency compared to the SMS case. However, as will be demonstrated in the following sections, the hybrid technique produces waveforms free from low-frequency harmonics, which represents a crucial advantage in various applications. For instance, in electrical drive systems, the presence of such harmonics poses a fundamental issue, as they directly impact torque ripple and the overall performance of the drive.

4. Simulation Results

Simulation results are presented in this Section to compare the performance of a 3-P 7-L ACHBMLI under different modulation techniques. The analysis primarily examines the harmonic distortion present in the output voltages and currents, providing insights into the performance of each modulation technique. It should be emphasized that each modulation technique is applied individually in simulation and HIL testing. The comparison focuses on an in-depth analysis of the harmonic content of the output voltages and currents. The system under study, shown in Figure 3, consists of a 3-phase, 7-level ACHBMLI connected to a passive load composed of a resistor in series with an inductor. The parameters of both the ACHBMLI and the load are provided in Table 1.

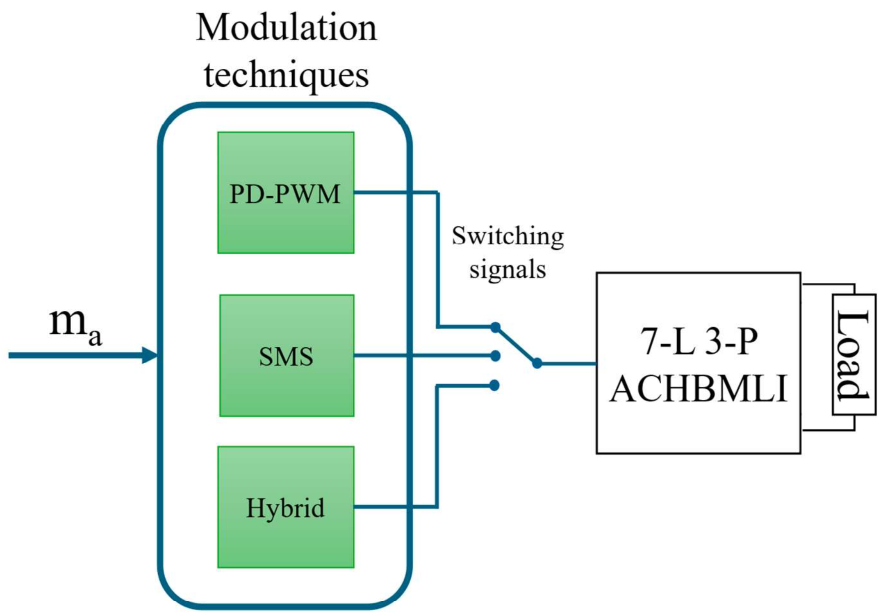

Figure 3. Block diagram of the modulation strategies applied to the 7-L 3-P ACHBMLI with a passive load.

Table 1. Data of ACHBMLI and passive load.

Symbol	Quantity	Value
V_{DC}	Voltage of DC generator	50 V
r_0	Power supply circuit resistance	0.1 Ω
L_0	Power supply circuit inductance	1 µH
C	DC-link capacitance	2.2 mF
f_{sw}	Carrier frequency	10 kHz
t_d	Dead time	1 µs
R	Resistance load	10 Ω
L	Inductance load	3 mH

The comparison is carried out by analyzing the output voltage waveform corresponding to each modulation technique. A key aspect of the evaluation is the harmonic spectrum of both voltage and current, along with their THD, which is essential for assessing power quality. The simulations were performed using a MATLAB/Simulink R2024b model, enabling an accurate representation of the system's behavior under various modulation strategies.

A key factor analyzed in this study is the quality of the output voltage waveform generated by the 7-level three-phase ACHBMLI. Figure 4 presents a comparison of the voltage waveforms and their corresponding harmonic spectra for the three implemented modulation techniques. The analysis was conducted under operating conditions with a modulation index (m_a) of 0.95, chosen to represent a relevant and practical scenario for evaluating both harmonic content and overall waveform quality across different modulation strategies. However, the fundamental frequencies, as well as the frequency of the modulation signal, are equal to 50 Hz, whereas the switching frequency depends on the modulation technique used. For instance, with SMS the switching frequency is equal to the fundamental frequency, while for PWM it depends on the carrier frequency, which in this case is 10 kHz.

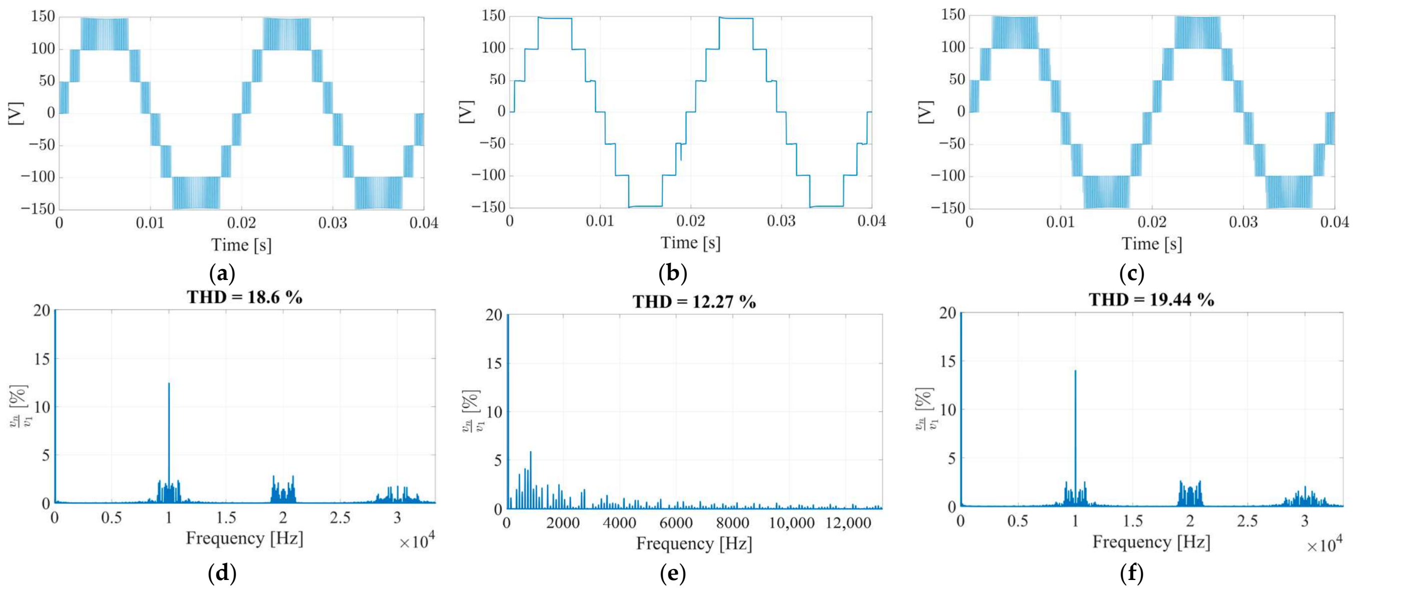

Figure 4. Waveforms and harmonic spectra of the voltage for the analyzed modulation techniques: (**a**) PD-PWM voltage, (**b**) SMS voltage, (**c**) hybrid voltage, (**d**) harmonic spectrum of PD-PWM, (**e**) harmonic spectrum of SMS, (**f**) harmonic spectrum of the hybrid technique.

The voltage phase waveforms are shown in Figure 4a–c. It can be observed that the waveform produced by the SMS technique features fewer switching transitions and is composed of well-defined voltage steps. In contrast, both PWM and hybrid techniques result in waveforms with a greater number of pulses. This difference stems from the switching frequency: SMS operates at a lower switching frequency, resulting in fewer transitions, while PWM and hybrid techniques employ higher switching frequencies, producing smoother and more refined voltage waveforms.

The corresponding harmonic spectra, depicted in Figure 4d–f, reveal significant differences in harmonic distribution among the three techniques.

The PWM spectrum is dominated by high-frequency harmonics, primarily concentrated around multiples of the modulation frequency (10 kHz), although some low-frequency components are still present. Conversely, the SMS technique introduces predominantly low-frequency harmonics, which may adversely affect system performance especially in sensitive applications such as electric drives. The HBR spectrum closely resembles that of PWM but exhibits a notable reduction in low-frequency harmonics, offering a more balanced trade-off between harmonic performance and switching losses.

The THD values of the output voltage for the PWM, SMS, and hybrid techniques are 18.6%, 12.27%, and 19.44%, respectively. At first glance, SMS seems to provide the best harmonic performance, as it yields the lowest THD value.

Indeed, as shown in Figure 5, the high-frequency harmonics are effectively filtered out by the load, leaving only the low-frequency components in the current waveform. As a result, the total harmonic distortion (THD) of the current supplied to the load when using SMS is 6.288%, whereas high-frequency modulation techniques achieve significantly lower values 0.949% for PWM and 1.008% for the hybrid technique. This confirms that while PWM and HBR generate harmonics primarily at higher frequencies, which are easier to attenuate, SMS introduces dominant low-frequency harmonics. This behavior is particularly advantageous in grid-connected applications, where strict power quality standards must be met, and high-frequency harmonics are more easily filtered by grid interface components, ensuring compliance with regulatory limits.

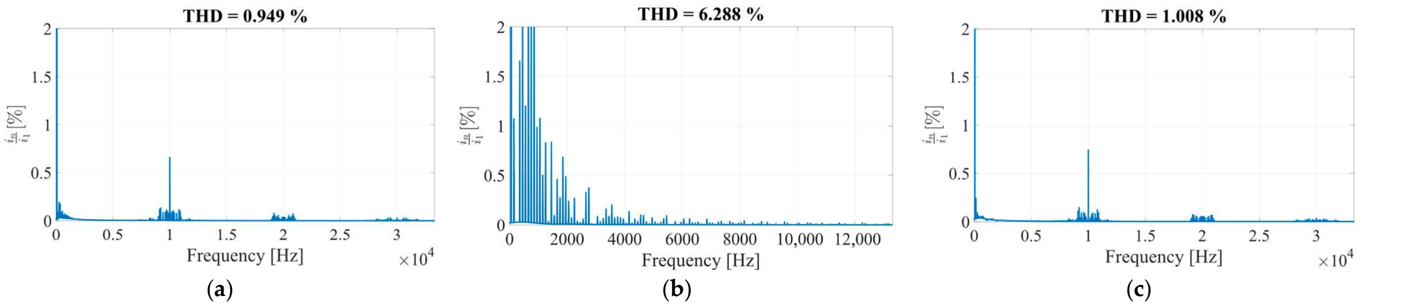

Figure 5. Harmonic spectra of the current for the analyzed modulation techniques: (**a**) PD-PWM, (**b**) SMS, (**c**) hybrid technique.

5. Description of the Test Bench Equipment

This section overviews the test bench equipment utilised for real-time validation. Specifically, as illustrated in Figure 6, the controller is installed on the Power Electronics and Drive (PED) Board V4 (Elettronica Dedicata Inc.), whose main specifications are detailed in Table 2.

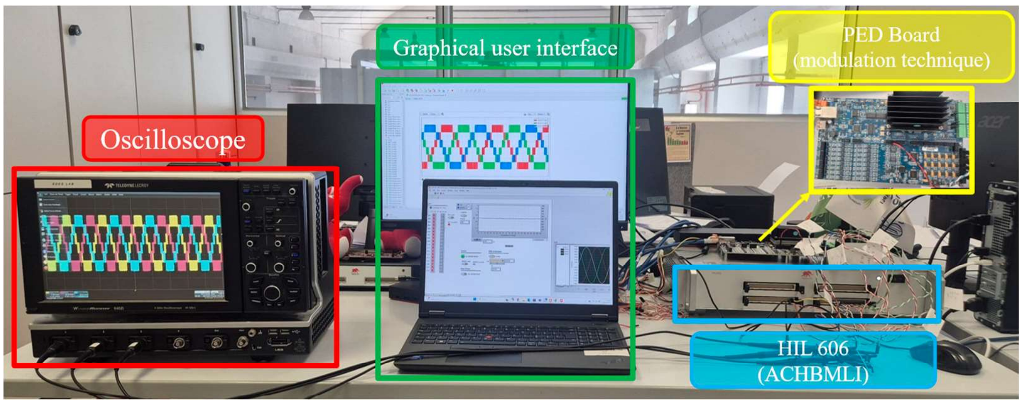

Figure 6. Test bench equipment.

Table 2. PED-Board V4 characteristics.

Hardware	Features
30×, 0÷15 V or 0÷5 V selectable voltage	PWM Channels
8 channels, Simultaneous sampling of 1.45 µs conversion time, 8 channels o Differential input o −5 V÷5 V or 0 V÷10 V configurable inputs magnetic induction	14 bit-ADC
8 channels, Simultaneous sampling of 1.45 µs conversion time, 8 channels of Differential input o −5 V÷5 V or 0 V÷10 V configurable inputs	14-bit-ADC
8 channels, up to 200 kS/s	10 bit-ADC
46 × 3.3 V standard	Digital I/O
programming, debugging, and operation	Ethernet

The modulation techniques are fully implemented using the LabVIEW graphical programming environment. The control architecture is structured into two fully parallel processing units. The first unit operates at high frequency and manages the modulator, including carrier signal generation, dead-time insertion, and gate signal production. The second unit is dedicated to data acquisition and modulation signal processing.

System initialization is synchronized to ensure that data sampling and control actions are triggered precisely at the peak and valley points of the carrier waveform. Consequently, the effective sampling frequency is twice the virtual switching frequency.

The 7-L 3-P ACHBMLI and the passive load under test are simulated in real time using the Typhoon HIL 606 Hardware-in-the-Loop platform. The scheme implemented in the HIL 606 is shown in Figure 6. The HIL 606 receives the switch control signals from the PED-Board, which allows the output voltage and current of the 7-L 3-P ACHBMLI, implemented directly within the HIL 606, to be generated in real time. The main features of this system are summarized in Table 3. For enhanced realism, the ACHBMLI has been fully integrated into the HIL environment to enable accurate real-time emulation. Moreover, this system allows loading the datasheet parameters of the electronic components to emulate their behavior. This capability makes it possible to estimate the converter losses, enabling the determination of the ACHBMLI efficiency and the analysis of its variation with different modulation techniques.

Table 3. HIL 606 characteristics.

Hardware	Features
ZU4EG Ultrascale + Zynq SoC	up to 8 processing cores
Analog Inputs (AI)	32×, up to 1 MSPS, ±10 V
Analog Outputs (AO)	64×, up to 5 MSPS, ±10 V
Digital Inputs (DI)	64×, ±15 V
Digital Outputs (DO)	64×, 0÷5 V
Ethernet	4× RJ45; up to 1000 Mbps

6. Real-Time Validation

In this section, the real-time validation of the modulation strategies under investigation was performed. For each experimental trial, the microcontroller was reset and the subsequent modulation technique was initialised.

Specifically, several real-time validation tests were conducted using the test bench shown in Figure 7 to compare the harmonic content of the generated voltages and currents, their THD and the efficiency of the power converter. Furthermore, with the HIL 606 platform, it is possible to monitor the temperature of each ACHBMLI component, enabling the study of thermal behaviour under different modulation techniques and assessing the thermal stress experienced by the power devices. Additionally, the parameters of the passive load and the ACHBMLI are the same as those in the previous Section 4, as described in Table 1.

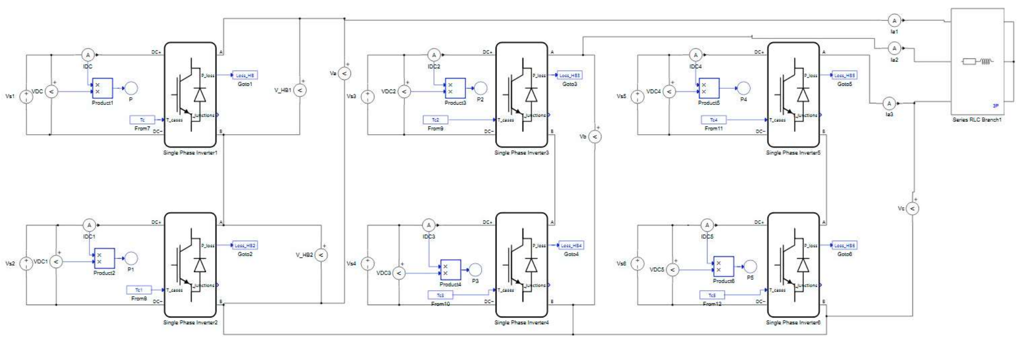

Figure 7. 7-L 3-P ACHBMLI implemented in the HIL606.

It is essential to analyse the voltage spectra for the three modulation techniques. The spectral analysis provides deeper insight into the harmonic content of the generated waveforms, highlighting the impact of each modulation strategy on power quality. In the following section, the voltage spectra obtained from real-time validation are compared to assess the distribution of harmonics and their effects on the system. In this case, the reported line voltages are relative to operating conditions in which the modulating index is slightly less than one, precisely equal to 0.95.

Figure 8 shows the waveforms of the line voltages and their respective spectra. In the case of PWM, the spectrum primarily contains harmonics multiples of the switching frequency (10 kHz), which are easily filtered by the load. Conversely, the SMS modulation spectrum exhibits significant low-frequency harmonics, while those above 10 kHz are of negligible magnitude. Particularly interesting is the analysis of Figure 8c, which relates to the hybrid technique: Although the HBb bridge switches at the fundamental frequency, the only harmonics present are multiples of 10 kHz, similar to PWM. The THD values of the output voltage for the PD-PWM, SMS, and hybrid techniques are 18.6%, 12.2%, and 19.44%, respectively.

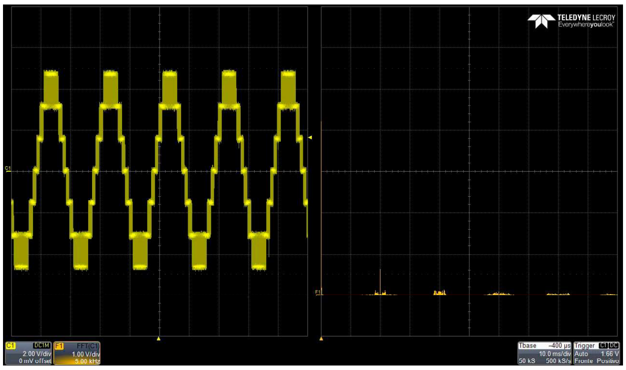

(**a**)

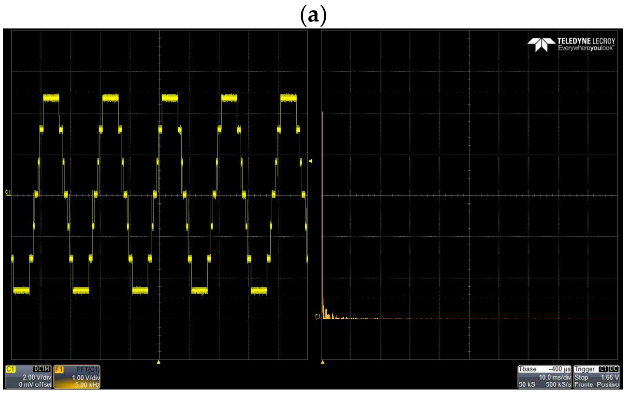

(**b**)

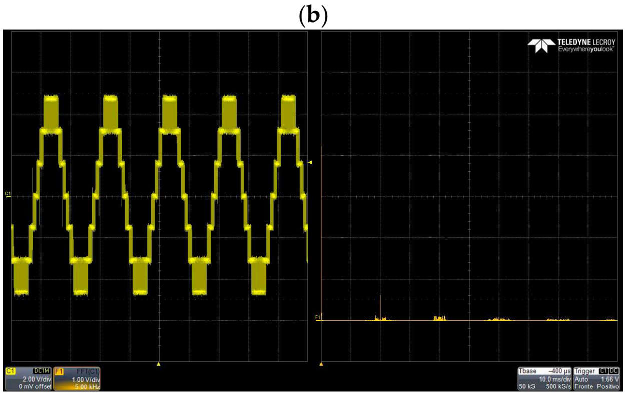

(**c**)

Figure 8. Waveforms and harmonic spectra of the voltage for the evaluated modulation techniques in real-time validation: (**a**) PD-PWM, (**b**) SMS, (**c**) hybrid.

Indeed, as shown in Figure 9, the high-frequency harmonics are effectively filtered out by the load, leaving only the low-frequency components in the current waveform. As a result, the THD of the current supplied to the load when using SMS is 6.288%, whereas high-frequency modulation techniques achieve significantly lower values 0.949% for PWM and 1.008% for the hybrid technique. This confirms that while PWM and HBR generate harmonics primarily at higher frequencies, which are easier to attenuate, SMS introduces dominant low-frequency harmonics.

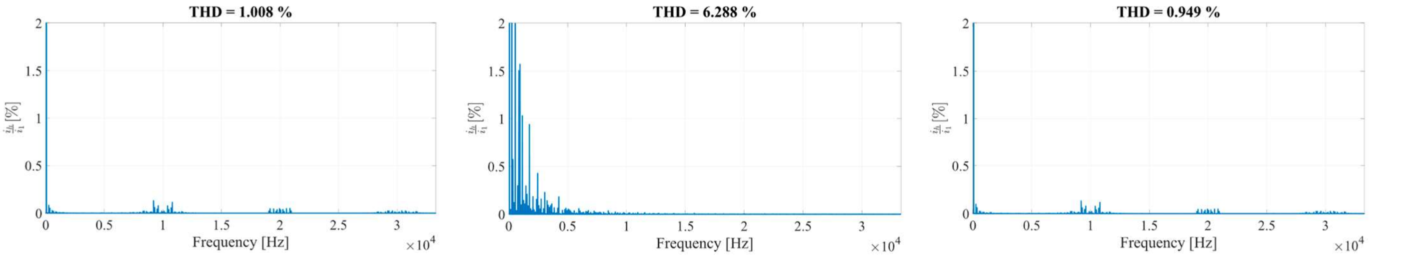

(**a**) (**b**) (**c**)

Figure 9. Harmonic spectra of the load current for the evaluated modulation techniques in real-time validation: (**a**) PD-PWM, (**b**) SMS, (**c**) hybrid technique.

Additionally, an extensive series of tests was performed to compare the three modulation techniques in terms of voltage THD (THD_V), current THD (THD_I), and efficiency (η) of the ACHBMLI. The assessment was conducted under various operating conditions, with a m_a ranging from 0.2 to 1, comprehensively evaluating each technique's performance.

Additional tests were carried out to evaluate how the voltage and current vary following a change in load, specifically when the load is halved while maintaining a constant power factor. The results are presented in Figure 10. As can be observed, when the load is reduced, the voltage remains constant and is not affected by the variation, whereas the current increases for all modulation techniques. It should also be noted that no substantial differences are observed among the modulation techniques.

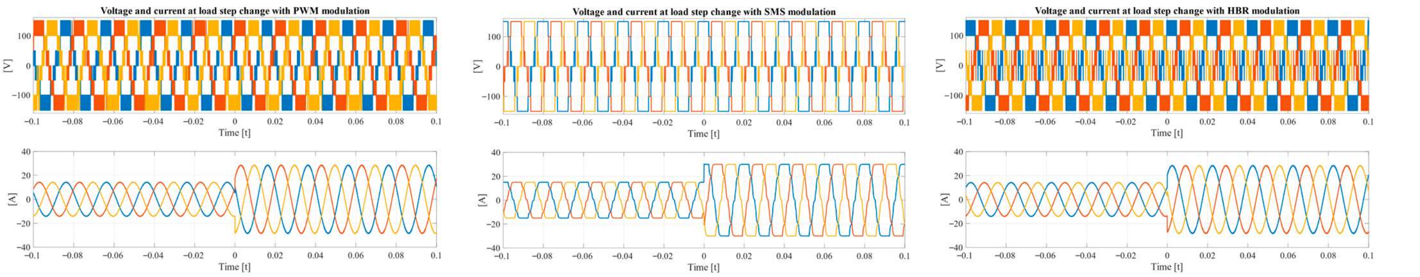

(**a**) (**b**) (**c**)

Figure 10. System step response as the modulation technique changes: (**a**) PD-PWM, (**b**) SMS, (**c**) hybrid technique.

In Figure 11, the THD values of both voltage and current THD are shown for different operating. Generally, regardless of the modulation strategy employed, increasing the modulation index results in a reduction in both THD_V and THD_I. It can generally be stated that the SMS technique achieves better harmonic performance, especially at higher ma values, although the results remain comparable to those of the other two modulation methods. PWM and the hybrid approach consistently yield almost identical THD_V values.